

1 Stochastic Modeling of Soil Salinity

S. Suweis, A. Rinaldo, S.E.A.T.M. Van der Zee, E. Daly, A. Maritan,

and A. Porporato

S. Suweis, Laboratory of Ecohydrology ECHO/IEE/ENAC/EPFL, École Polytechnique Fédérale, Station 2, GR C1 515, Lausanne(CH)

A. Rinaldo, Laboratory of Ecohydrology ECHO/IEE/ENAC/EPFL, Lausanne (CH) and Dipartimento IMAGE, Università di Padova, Padova (IT)

E. Daly, Department of Civil Engineering, Monash University, Clayton, VIC (AU) and National Centre for Groundwater Research and Training, Flinders University, Adelaide (AU)

S.E.A.T.M. Van der Zee, Soil Physics, Ecohydrology and Groundwater Management, Environmental Sciences Group, Wageningen University, Wageningen (NE)

A. Maritan, Dipartimento di Fisica Galileo Galilei, Università di Padova, Padova (IT)

A. Porporato, Department of Civil and Environmental Engineering, Duke University, Durham, NC (USA)

arXiv:1207.2332v1 [physics.geo-ph] 10 Jul 2012

2 A minimalist stochastic model of primary soil salinity is proposed, in which
3 the rate of soil salinization is determined by the balance between dry and
4 wet salt deposition and the intermittent leaching events caused by rainfall
5 events. The long term probability density functions of salt mass and concen-
6 tration are found by reducing the coupled soil moisture and salt mass bal-
7 ance equation to a single stochastic differential equation driven by multiplica-
8 tive Poisson noise. The novel analytical solutions provide insight on the in-
9 terplay of the main soil, plant and climate parameters responsible for long-
10 term soil salinization. In particular, they show the existence of two distinct
11 regimes, one where the mean salt mass remains nearly constant (or decreases)
12 with increasing rainfall frequency, and another where mean salt content in-
13 creases markedly with increasing rainfall frequency. As a result, relatively
14 small reductions of rainfall in drier climates may entail dramatic shifts in long-
15 term soil salinization trends, with significant consequences e.g. for climate
16 change impacts on rain-fed agriculture.

1. Introduction

17 Large areas of cultivated land worldwide are affected by soil salinity. *Szabolcs* [1989]
18 estimates that 10% of arable land in over 100 countries, and nine million km² are salt
19 affected, especially in arid and semi-arid regions [*Tanji*, 1989]. Salinity refers to large
20 concentrations of easily soluble salts present in water and soil on a unit volume or weight
21 basis (typically expressed as electrical conductivity (EC) of the soil moisture in dS/m,
22 i.e. deciSiemens per meter at 25° C; for *NaCl* 1 mg/l $\sim 15 \cdot 10^{-4}$ dS/m). High salinity
23 causes both ion specific and osmotic stress effects, with important consequences for plant
24 production and quality. Normally, yields of most crops are not significantly affected if
25 EC ranges from 0 to 2 dS/m, while above levels of 8 dS/m most crops show severe yield
26 reductions [*Ayars et al.*, 1993; *Hillel*, 2000]. Prevention or remediation of soil salinity
27 is usually done by leaching salts, and has resulted in the concept of leaching require-
28 ment [*Richards*, 1954; *Hillel*, 1998; *Schleiff*, 2008]. Alternative amelioration strategies by
29 harvesting salt-accumulating plants appear to be less effective [*Qadir et al.*, 2000].

30 Salt accumulation in the root zone may be due to natural factors (primary salinization)
31 or due to irrigation (secondary salinization). Several detailed numerical models have been
32 developed to model soil salinization [e.g. *Eldin et al.*, 1987; *Schoups et al.*, 2006; *Corwin*
33 *et al.*, 2007]. Generally, these models simulate unsaturated soil water flow via Richards
34 and solute transport equations. These models are more suitable for local and short-term
35 simulations, as they require precise soil characterization and are computationally demand-
36 ing. Moreover, it is often difficult to identify cause-effect relationships or to synthetically
37 compare the effects of different parameter scenarios from their numerical simulations.

38 Vertically-averaged soil moisture and salt balance equations have also been used [*Allison*
39 *et al.*, 1994; *Hillel*, 2000]. Despite their simplicity, these models have the advantage of
40 parsimony, thus allowing a direct analysis of the interplay of the main processes, and
41 provide an ideal starting point to include external, random hydroclimatic fluctuations
42 in the analysis of long-term salinization trends. The goal of this Letter is to offer a
43 first step in this direction. With this purpose, here we present a minimalist model of
44 soil primary salinization, describing analytically the long-term dynamics of salt in soils
45 caused by wet (rain) and dry (aerosol) deposition. Our aim is to quantify the salt mass and
46 concentration probability density functions (pdfs) in the root zone, and the probability
47 of crossing the crops salt tolerance threshold as a function of the main hydro-climatic
48 parameters. The model framework is potentially extendible to systems including salt
49 input from groundwater and irrigation.

2. Methods

50 Our starting point is a spatially lumped model [*Bras and Seo*, 1987] for the vertically
51 averaged dynamics of soil moisture and salt in the root zone. As a first step we will not
52 consider input of salt due by irrigation or groundwater upflow. Following *Rodriguez-Iturbe*
53 *et al.* [1999], *Rodriguez-Iturbe and Porporato* [2004] and *Porporato et al.* [2004], rainfall
54 (R_t) is modeled as a marked point process with frequency λ_p and with daily rainfall
55 depths exponentially distributed with mean $1/\gamma_p$. The averaged soil moisture dynamics
56 are modeled assuming constant (spatially and temporally averaged) soil and ecohydrolog-
57 ical parameters, i.e., root depth, Z_r , porosity, n , and maximum evapotranspiration rate,
58 ET_{max} . Assuming a rain salt concentration C_R and a constant input \mathcal{M}_d of salt mass per

59 unit ground area and per unit time by dry deposition, the root-zone mass balance for soil
 60 moisture and salt mass m is given by:

$$nZ_r \frac{ds}{dt} = -ET(s) - L(s) + R_t, \quad (1)$$

$$\frac{dm}{dt} = C_R R_t + \mathcal{M}_d - CL(s), \quad (2)$$

61 where C is the salt concentration in the root zone; $L(s)$ represents deep percolation, while
 62 $ET(s)$ represents the losses resulting from plant transpiration and soil evaporation. As
 63 in *Porporato et al.* [2004], $ET(s)$ is assumed to be linear in the range of soil moisture
 64 comprised between the wilting point, s_w , and a suitable soil moisture threshold s_1 (an
 65 effective field-capacity threshold), at which ET occurs at the maximum rate ET_{max} . All
 66 the rainfall input that cannot be accommodated is assumed to be lost as $L(s)$ at s_1 . In
 67 this minimalist model the effect of salt-induced changes in osmotic potential may only
 68 indirectly be taken into account through an average reduction of ET_{max} . This is simply
 69 done here by keeping the same ET_{max} for the two models (previous studies [*Viola et al.*,
 70 2008] have shown that, in the absence of osmotic effects, the minimalist model should have
 71 artificially higher ET_{max} to account for percolation losses below s_1). A full account of how
 72 reduction in evapotranspiration affects salinization patterns (reduced evapotranspiration
 73 in turn increases the available soil moisture and thus reduces the concentration of salt in
 74 the soil and increases leaching frequencies) will be given elsewhere.

75 A complete numerical model, in which the impact of osmotic stress in reducing ET is
 76 explicitly included [*Bras and Seo*, 1987], has been also studied. Moreover, in the detailed
 77 model runoff takes place at saturation ($s = 1$), while percolation occurs for $s > s_{fc}$ (the soil
 78 moisture field capacity), and it is proportional to the soil hydraulic conductivity $K_{sat}s^c$,

79 where c is a soil-pore connectivity index and K_{sat} is the saturated hydraulic conductivity
 80 [*Rodriguez-Iturbe and Porporato, 2004*]. A comparison between the results of the two soil
 81 moisture models, presented in Figure 1a, suggests the viability of the simplified model.
 82 Simulations for wetter climates confirm this result.

83 The system (1) and (2) can be further simplified if one considers that the typical
 84 timescales for salt mass dynamics in the root zone are orders of magnitude larger than the
 85 ones characterizing rainfall (and thus wet deposition). Moreover, soil moisture typically
 86 reaches steady-state conditions within a growing season (e.g., $< 5 - 7$ months), while the
 87 salt mass balance only does so on much longer times scales (e.g., $>$ decades). Accordingly,
 88 at those long timescales, say T , the salt mass input flux can be assumed to take place
 89 at a constant rate, Υ , that is $\int_t^{t+T} (\mathcal{M}_d + C_R R_t) dt' \sim \mathcal{M}_d T + T C_R \lambda_P / \gamma_P = \Upsilon T$, and be
 90 interrupted by instantaneous and unfrequent leaching events induced by percolation. As
 91 a result, (2) can be rewritten as

$$\frac{dm}{dt} = \Upsilon - \frac{m}{n Z_r s} L(s). \quad (3)$$

92 Leakage may then be modelled as a marked point process, with percolation depths ex-
 93 ponentially distributed with parameter γ_P [*Botter et al., 2007*]. For reasons of analytical
 94 tractability, the percolation events are assumed to occur according to a Poisson process
 95 with frequency λ given by the frequency of soil moisture crossing the threshold $s = s_1$.
 96 This can be expressed in terms of the soil moisture pdf as $\lambda = \rho(s_1)p(s_1)$, where the
 97 term $\rho(s) = (ET(s) + L(s))/nZ_r$ represents the normalized catchment-scale loss function
 98 (i.e. the total losses from the system due to evapotranspiration and leakage as a function
 99 of the soil moisture) [*Rodriguez-Iturbe and Porporato, 2004*]. Adopting the soil moisture

100 minimalist model (for which the pdf is a truncated gamma distribution, e.g., *Porporato*
 101 *et al.* [2004]), the leaching frequency is $\lambda = \eta \exp(-\gamma) \gamma^{\lambda_P/\eta} / \Gamma(\lambda_P/\eta, \gamma)$ [*Botter et al.*,
 102 2007], where $\Gamma(x, y)$ is the lower incomplete gamma function, $\eta = ET_{max}/(nZ_r(s_1 - s_w))$
 103 and $\gamma = \gamma_P nZ_r(s_1 - s_w)$.

104 A leaching-efficiency parameter b is used to account for incomplete salt dissolution,
 105 further assuming that the typical value of soil moisture during leaching events can be
 106 approximated by the value s_1 . With the above assumptions, the dynamics of the salt
 107 mass in the root zone can be described by a single equation

$$\frac{dm}{dt} = \Upsilon - mL'_t, \quad (4)$$

108 where L'_t is a marked Poisson noise [*Van Den Broeck*, 1983] with frequency λ , and (di-
 109 mensionless) exponential marks with mean

$$\mu = \frac{b}{nZ_r s_1 \gamma_P}. \quad (5)$$

110 Figures 1b and 1c compare the results of both salinity models. The free parameters
 111 s_1 and b are fitted with respect to the complete model of salt mass and concentration,
 112 respectively.

113 From a mathematical viewpoint, equation (4) is a stochastic differential equation with
 114 multiplicative white (jump) noise. In our case, since the soil solution can be considered in
 115 equilibrium during leaching events, one has to interpret (4) in the Stratonovich sense [*Van*
 116 *Den Broeck*, 1983]. Accordingly, the normal rules of calculus are preserved, and equation
 117 (4) can be transformed into

$$\frac{dy}{dt} = \Upsilon e^{-y} - L'_t, \quad (6)$$

118 where $y(t) = \ln[m(t)]$.

3. Results and Discussion

119 The stationary solution of (6) can be obtain as in *Rodriguez-Iturbe et al.* [1999]. Then
 120 using the derived distribution for m , i.e., $p(m) = p(y)dy/dm$, we obtain the probability
 121 distribution for the salt mass in the root zone

$$p(m) = \mathcal{N} \exp\left(-\frac{m\lambda}{\Upsilon}\right) m^{1/\mu}, \quad (7)$$

122 where $\mathcal{N} = (\lambda/\Upsilon)^{\frac{1+\mu}{\mu}}/\Gamma(\frac{1+\mu}{\mu})$ and $\Gamma(x)$ is the Gamma function. Equation (7) summarizes
 123 the soil salinity statistics as a function of climate, soil and vegetation parameters.

124 Figure 2 is a graphical representation of the dependence of the mean salt concentration
 125 $\langle C \rangle = \langle m \rangle / nZ_r \langle s \rangle$ on the yearly rainfall and λ_p . The contour-lines connect equal values
 126 of the mean salt concentration in the soil, for a given input of salt Υ . The latter has been
 127 calculated for two different geographic regions. Typical salt inputs in coastal areas are
 128 100 – 200 kg/(ha yr) of salt, while values drop of an order of magnitude in continental
 129 regions [*Hillel*, 2000].

130 Between the black region and the light gray ones in Figure 2a, the behavior of $\langle C \rangle$
 131 changes substantially. Above a certain total rainfall per year, the input of salt related
 132 to rainfall frequency becomes immaterial as leaching effectively washes out the salt mass
 133 from the root zone. For lower total rainfall values, however, the salt in the soil increases
 134 with increasing λ_p . For a given annual precipitation depth, with low rainfall frequencies,
 135 rainfall events carry enough water to trigger leaching. Conversely, if λ_p is high, evapo-
 136 transpiration dominates, leaching is largely reduced, thereby causing salt accumulation
 137 in the root zone. Therefore, $\langle m \rangle$ strongly increases with λ_p . Relatively small reductions

138 of rainfall at the transition between these two regimes may entail a dramatic increase in
 139 long-term soil salinization. Figure 2 also shows the threshold of soil salinity below which
 140 vegetation is practically unaffected (e.g., $\langle C \rangle < 2$ dS/m) and the thresholds above which
 141 regular (e.g. non-halophytic) vegetation is damaged (e.g., $\langle C \rangle > 2$ dS/m). For coastal
 142 areas soil salinization may occur even in relatively more humid regions, especially when
 143 rainfall events are not very intense. On the contrary, in continental regions only arid
 144 climates may begin to develop soil salinization (in the absence of irrigation and ground-
 145 water input). Indeed, through our model one can evaluate the risk of soil salinization in
 146 rain-fed agriculture just by estimating the typical salt inputs, total rainfall per year and
 147 the rainfall frequency. For example, a rain-fed crop in a semi-arid climate (e.g., rainfall
 148 depth of 70 cm/yr) in a continental region risks salinization only when rainfall events are
 149 not very intense (e.g., $\gamma_p^{-1} \leq 0.4$ cm or $\lambda_p \geq 0.48$ d $^{-1}$). If the same crop is located in a
 150 coastal area, salinization occurs for a wider range of rainfall parameters (e.g., $\gamma_p^{-1} \leq 1$ cm
 151 or $\lambda_p \geq 0.18$ d $^{-1}$).

152 The solution (7) may be used in conjunction with soil moisture statistics to obtain a full
 153 characterization of the salt concentration in the root zone. Because one may safely assume
 154 that equations (1) and (3) are decoupled over short time scales, the soil moisture $s(t)$
 155 and the salt mass $m(t)$ may be treated as statistically independent random variables. By
 156 observing that the salt concentration in the root zone is equal to $C(t) = m(t)/nZ_r s(t)$ and
 157 assuming $s_w \sim 0$, we find the stationary probability distribution of the salt concentration

158 $p(C)$ as the quotient distribution of two independent random variables [*Curtiss*, 1941],

$$p(C) = \frac{\lambda \left(\frac{\Upsilon \gamma_P}{C\lambda} + 1\right)^{-1/\mu} \left(\frac{\Upsilon \gamma_P}{C\lambda + \Upsilon \gamma_P}\right)^{\frac{\lambda_P}{\eta}} \left(\Gamma\left(\frac{\lambda_P}{\eta} + \frac{1}{\mu} + 1\right) - \Gamma\left(\frac{\lambda_P}{\eta} + \frac{1}{\mu} + 1, nZ_r s_1 \left(\frac{C\lambda}{\Upsilon} + \gamma_P\right)\right)\right)}{\Gamma\left(1 + \frac{1}{\mu}\right) (C\lambda + \gamma_P \Upsilon) \left(\Gamma\left(\frac{\lambda_P}{\eta}\right) - \Gamma\left(\frac{\lambda_P}{\eta}, nZ_r s_1 \gamma_P\right)\right)}. \quad (8)$$

159 The comparison between analytical solutions and numerical simulations (Figure 3) shows
160 that the analytical solution reproduces reasonably well the pdf of the complete model.

161 By integrating equation (8) from a given concentration value C^* to infinity, one obtains
162 the cumulative pdf of C , $P(C^*)$, which is the probability of having a salt concentration
163 greater than a certain critical concentration value, C^* , as a function of the soil-plant-
164 atmosphere parameters. The inset of Figure 3 confirms the impact that climate change
165 may have on soil salinity. Note, in particular, that such an impact is marked only for
166 semi-arid or drier climates (see Figure 2). For example with a reduction from $\lambda_P = 0.2$
167 to $\lambda_P = 0.15 \text{ d}^{-1}$, the probability of crossing $C^* = 6 \text{ dS/m}$ is more than tripled. When
168 coupled to a crossing analysis of concentration levels, the previous results may be used to
169 evaluate the risk of plant salt stress. The analytical form of the results makes it suitable for
170 computations of salinity risk at the global scale as a function of few measurable parameters,
171 and facilitates their coupling with other models of long-term soil-plant biogeochemistry.

4. Conclusions

172 In this Letter we have presented an analytical approach to stochastic modeling of soil
173 salinity, where the complexity of the problem is reduced by employing simplifying assump-
174 tions that permit us to describe high-dimensional, unpredictable components via suitable
175 random terms. By assuming time-averaged inputs of salt and instantaneous percolation

176 processes, a decoupling from soil moisture equation results in a simplified stochastic mass
177 balance equation for the soil salt mass amenable to exact solution.

178 Soil salinity statistics are obtained as a function of climate, soil and vegetation parame-
179 ters. These can be combined with soil moisture statistics to obtain a full characterization
180 of soil salt concentrations and the ensuing risk of primary salinization.

181 This modeling framework can be extended to investigate additional salt inputs from
182 irrigation and groundwater by modifying accordingly the average salt input parameter Υ
183 and calculating the corresponding soil moisture pdfs (e.g. see *Vervoort and Van Der Zee*
184 [2008] for groundwater inputs and *Vico and Porporato* [2009] for irrigation).

185 **Acknowledgments.** This research is supported by funds provided by the ERC Ad-
186 vanced Grant RINEC-227612 and by SFN grant 200021_124930/1. AM acknowledges
187 funds provided by Fondazione Cariparo (Padova, IT). AP acknowledges the support of
188 the Landolt & Cie visiting chair "Innovative Strategies for a Sustainable Future" at the
189 EPFL (CH) and the collaboration grant with US Department of Agriculture, Agricultural
190 Research Service, Temple, TX; SvdZ acknowledges the hospitality of ENAC/EPFL for his
191 sabbatical stay. ED acknowledges the support of the Australian Research Council and the
192 Australian National Water Commission.

References

193 Allison, G., G. Gee, and S. Tyler (1994), Vadose-zone techniques for estimating ground-
194 water recharge in arid and semiarid regions, *Soil Sci. Soc. Am.*, (58), 6–14.

- 195 Ayars, J., R. Hutmacher, R. Schoneman, S. Vail, and T. Pflaum (1993), Long-term use
196 of saline water for irrigation, *Irr. Science*, *14*(1), 27–34.
- 197 Botter, G., A. Porporato, I. Rodriguez-Iturbe, and A. Rinaldo (2007), Basin-scale soil
198 moisture dynamics and the probabilistic characterization of carrier hydrologic flows:
199 Slow, leaching-prone components of the hydrologic response, *Water Resour. Res.*, *43*(2).
- 200 Bras, R., and D. Seo (1987), Irrigation control in the presence of salinity: Extended linear
201 quadratic approach, *Water Resour. Res.*, *23*(7).
- 202 Corwin, D., R. J.D., and J. Simunek (2007), Leaching requirement for soil salinity control:
203 Steady-state versus transient models, *Agric. Water Manag.*, (90), 165–180.
- 204 Curtiss, J. (1941), On the distribution of the quotient of two chance variables, *Annals Of*
205 *Mathematical Statistics*, *12*, 409–421.
- 206 Eldin, M., I. King, and K. Tanji (1987), Salinity management model. 1. Development, *J.*
207 *Irrig. Drain. Eng. A.*, *113*(4), 440–453.
- 208 Hillel, D. (1998), *Environmental Soil Physics*, Academic Press, London.
- 209 Hillel, D. (2000), *Salinity management for sustainable irrigation: Integrating science, envi-*
210 *ronment, and economics*, The International Bank for Reconstruction and Development,
211 the World Bank, Washington.
- 212 Porporato, A., E. Daly, and I. Rodriguez-Iturbe (2004), Soil water balance and ecosystem
213 response to climate change, *Am. Nat.*, *164*(5), 625–632.
- 214 Qadir, M., A. Ghafoor, and G. Murtaza (2000), Amelioration strategies for saline soils:
215 A review, *Land Degrad. and Develop.*, *11*(6), 501–521.

- 216 Richards, L. (1954), *Diagnosis and Improvement of Saline and Alkali Soils*, USDA Hand-
217 book No.60, Washington.
- 218 Rodriguez-Iturbe, I., and A. Porporato (2004), *Ecohydrology of Water Controlled Ecosys-*
219 *tems: Soil Moisture and Plant Dynamics*, Cambridge Univ. Press, New York.
- 220 Rodriguez-Iturbe, I., A. Porporato, L. Ridolfi, V. Isham, and D. Cox (1999), Probabilistic
221 modelling of water balance at a point: The role of climate, soil and vegetation, *Proc.*
222 *Roy. Soc. A.*, 455, 3789–3805.
- 223 Schleiff, U. (2008), Analysis of water supply of plants under saline soil conditions and
224 conclusions for research on crop salt tolerance, *J. Agron. Crop Science*, 194(1), 1–8.
- 225 Schoups, G., J. Hopmans, and K. Tanji (2006), Evaluation of model complexity and
226 space-time resolution on the prediction of long-term soil salinity dynamics, western San
227 Joaquin Valley, California, *Hydr. Processes*, 20(13), 2647–2668.
- 228 Szabolcs, I. (1989), *Salt-Affected Soils*, CRC Press, Boca Raton.
- 229 Tanji, K. (1989), Agricultural salinity - Nature, extent and concerns, in *National Water*
230 *Conference*, edited by Austin, TA, pp. 33–38.
- 231 Van Den Broeck, C. (1983), On the relation between white shot noise, gaussian white
232 noise, and the dichotomic markov process, *J. of Stat. Phys.*, 31(3), 467 – 483.
- 233 Vervoort, W., and S. E. A. T. M. Van Der Zee (2008), Simulating the effect of capillary
234 flux on the soil water balance in a stochastic ecohydrological framework, *Water Resour.*
235 *Res.*, 44(8), W08,425+.
- 236 Vico, G., and A. Porporato (2009), Traditional and micro-irrigation with stochastic soil
237 moisture, *Water Resour. Res.*, *in press*, doi:10.1029/2009WR008130.

238 Viola, F., E. Daly, G. Vico, M. Cannarozzo, and A. Porporato (2008), Transient soil
239 moisture dynamics and climate change in Mediterranean ecosystems., *Water Resour.*
240 *Res.*, *44*(11), W11,412.

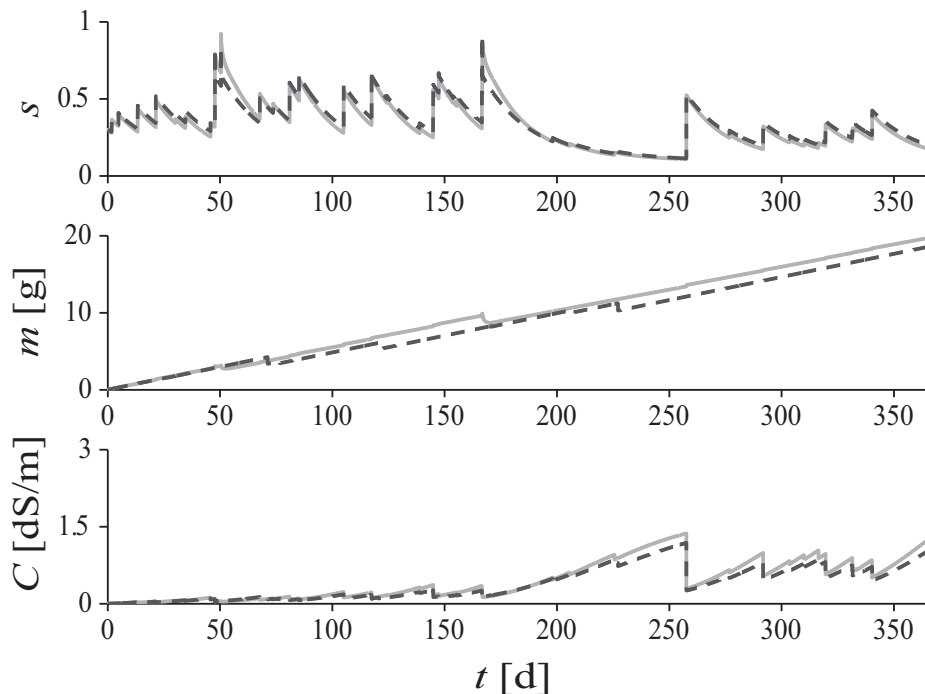


Figure 1. Comparison of soil moisture and salinity models: (a) Temporal evolution (equation (1)) of $s(t)$, forced by intermittent rainfall ($\lambda_p = 0.1 \text{ d}^{-1}$ and $1/\gamma_p = 1.79 \text{ cm}$). The blue dashed line refers to the minimalist model, while the continuous red line is the complete numerical model (see text for details). (b) Temporal evolution of root-zone salt mass for the complete numerical model (red line) and the minimalist model (blue dashed line). (c) Temporal evolution of the corresponding specific salt concentration $C(t) = m(t)/nZ_r s(t)$ in the root zone for the same two cases of 1b. We transform the unit of measure of C from $\text{mg}/(\text{cm m}^2)$ to dS/m , by using $\text{mg}/(\text{cm m}^2) = 10^{-1} \text{ mg}/\text{l}$. The soil and vegetation parameters employed for the simulation of the complete model are those typical for a sandy-loam soil, while the free parameters of the minimalist model are $s_1 = 0.8$, $b = 0.6$. In particular for both models we used $n = 0.45$, $Z_r = 30 \text{ cm}$, $s_w = 0.1$, $ET_{max} = 0.35 \text{ cm}/\text{d}$, $C_R \approx 3 \text{ mg l}^{-1}$ and $\mathcal{M}_d = 54 \text{ mg d}^{-1} \text{ m}^{-2}$ (coastal area).

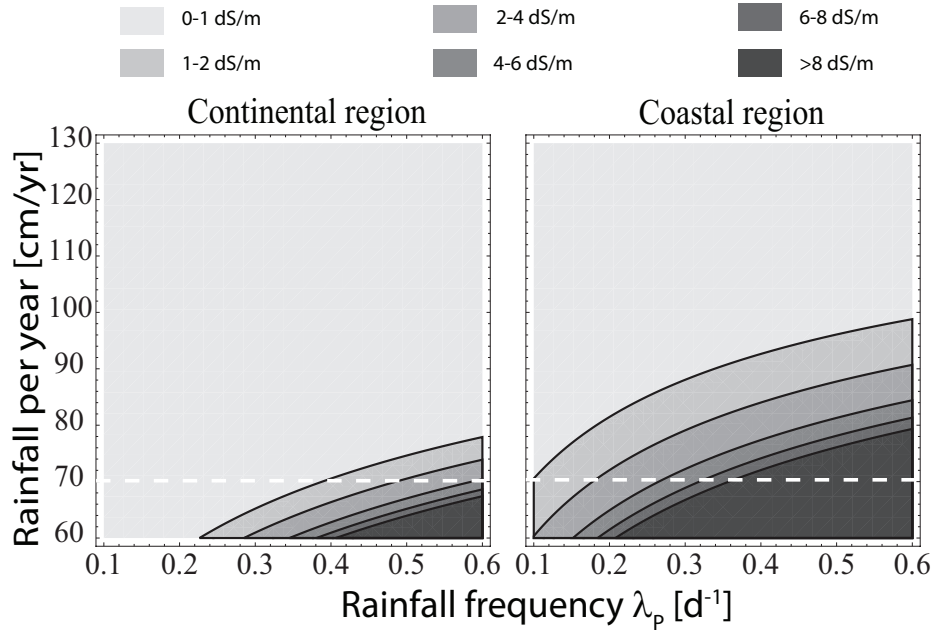


Figure 2. Contour plot of the asymptotic mean concentration of salt $\langle C \rangle$ from the exact solution of $\langle m \rangle$ as a function of yearly rainfall depth and frequency. The values reported in the legend refer to the corresponding salt concentration values with respect to the average soil moisture $\langle s \rangle$ (for its analytical expression see *Porporato et al.* [2004]). The contour lines represent significant soil salinity values (1,2,...,8 dS/m). The parameter μ has been calculated through equation (5); the others are as in Figure 1 for the coastal region, while for continental areas $\Upsilon \approx 6 \text{ mg d}^{-1} \text{ m}^{-2}$.

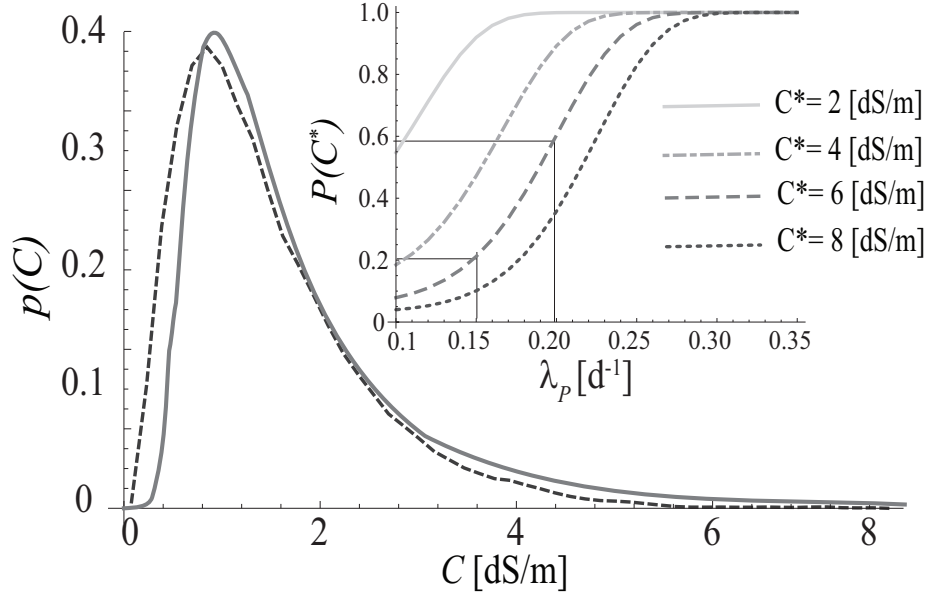


Figure 3. Comparison between the analytical form of $p(C)$ for the minimalist model obtained via equation (8) in which the free parameters (b and s_1) have been fitted (solid line) and the numerical simulations of the corresponding complete model (dashed line). The soil and hydro-climatic parameters are as in Figure 1. In the inset: probability of exceeding a soil salinization critical threshold C^* ($\int_{C^*}^{+\infty} p(C)dC$) as a function of the rainfall frequency λ_p .